Pak. J. Bot., 58(6) June, 2026.

ARTICLE | DOI: http://dx.doi.org/10.30848/PJB2026-6(10)

EFFECT OF NANOFORMULATION OF *NERIUM OLEANDER* (L.) AQUEOUS LEAVES –BASED IRON OXIDE NANOPARTICLES FOR THE CONTROL OF *TROGODERMA GRANARIUM* (COLEOPTERA: DERMESTIDAE)

OMAR HAMEED ABDULHADI[1*], ALI IRFAN ILBAS[2] AND FALAH ABOOD SABIT[3]

[1] Department of Agricultural Sciences and Technologies, Graduate School of Natural and Applied Science, Erciyes University, Kayseri, Türkiye
[2] Department of Field Crops, Faculty of Agriculture, Erciyes University, Kayseri, Türkiye
[3] Department of Plant Protection, College of Sciences Agriculture Engineering, University of Baghdad, Baghdad, Iraq
*Corresponding author's email: Hameedomer05@gmail.com

Abstract

Trogoderma granarium, commonly known as the khapra beetle, poses a significant threat to global food security due to its destructive impact on stored grains. This study aimed to assess the effectiveness of iron oxide nanoparticles biosynthesized from *Nerium oleander* leaves extract as a biological nano-insecticide. This approach offers a safe and natural alternative to chemical pesticides for controlling insects. The evaluation was conducted at various temperatures (25°C, 35°C, and 40°C) using several concentrations of nano iron oxide: 1000, 2000, 3000, and 4000 ppm. The exposure periods were set at 24, 48, and 72 hours. A direct method was employed to determine the impact of these nanoparticles on the egg, larval, pupal, and adult stages of the insect. The research specifically evaluated the effectiveness of iron oxide nanoparticles in preventing egg hatching. The highest inhibition rate was recorded at a concentration of 4000 ppm, reaching 100% at temperatures of 35°C and 40°C after 72 h of exposure. Additionally, these nanoparticles exhibited significant insecticidal activity against larvae under all tested conditions. At temperatures of 25°C and 35°C, larval mortality reached 100% at a concentration of 4000 ppm after 72 h. At 40°C, however, 100% mortality was achieved at a concentration of 3000 ppm after the same exposure period. Mortality rates for pupae at 4000 ppm were observed to be 50%, 73.66%, and 100% after 72 h at temperatures of 25°C, 35°C, and 40°C, respectively. The highest adult mortality, which reached 100%, was noted at 4000 ppm after 24 h at 35°C. These findings highlight the potential of *N. oleander* as an eco-friendly biocontrol agent for managing *T. granarium* infestations.

Key words: Iron Oxide Nanoparticles; Temperature; Larval mortality; Insecticidal activity

Introduction

Grains are one of the most essential food resources for humans, as they are rich in antioxidants, fiber, minerals, and vitamins. They also serve as the primary component of animal feed and have recently been utilized in bioenergy production through fermentation. Grains occupy 60% of the world's cultivated land. The most significant types of grains include wheat, rice, corn, and oats. (Hübner & Arendt, 2013). Grain crops are vulnerable to various insect infestations, both in the field and during storage. Stored agricultural products can be affected by over 600 species of beetles, 70 species of moths, and approximately 355 species of weevils. These infestations can lead to both quantitative and qualitative losses. (Rajendran & Anand, 2002; Sabit *et al*., 2025). It has been proven that the presence of insect residues in grains leads to an increase in the urea content in fine products, which are toxic substances. These residues are likely to cause changes in the grain components that may affect industrial processing and lead to milling difficulties. This is attributed to the Dermestidae family and the Coleoptera order, a polyphagous stored-food insect pest. They cause significant damage to stored foodstuffs from both economic and marketing perspectives, as they lead to weight loss of the stored materials, reduced nutritional value, and decreased germination rates of grains due to the larval stage feeding on cereal grains, particularly stored wheat. Additionally, secondary insect pests and fungi appear as a result of the infestation (Semple, 1992; Stathas *et al*., 2023), They are among the most resistant insects to chemical pesticides because they tend to enter a dormant state for a period of up to 3 years under unfavorable conditions (Saxena *et al*., 1992).

The inappropriate and excessive use of pesticides has resulted in the emergence of numerous insect species that have developed resistance, amounting to a total of 460 species by 2003. In addition to the risks posed by the development of resistance in pests and microorganisms, the high costs associated with chemical pesticide use represent another significant drawback (Brent, 1998; Nnadozie & Ajibade, 2020), targeting desirable natural enemies (Koul, 2008). Additionally, these residues contribute to environmental pollution, have detrimental biological impacts on human and animal health due to their limited biodegradability, and leave behind an unfavorable flavor and odor in stored grains (Alam, 1999; Mansoor-ul-Hasan *et al*., 2006; Ferencz & Balog, 2010).

The extracts are considered effective natural pesticides that can be employed in integrated pest management, crop protection, and the elimination of harmful economic insects. This effectiveness is largely due to the toxic compounds they contain, particularly phytochemicals such as diterpenoids and alkaloids, which exhibit toxic biological activity, induce cell death, and possess anti-nutritional properties.

Received: 04-09-2025 | Revised: 06-01-2026 | Accepted: 10-01-2026 | Online: 25-02-2026

To enhance the effectiveness of pesticides, nanotechnology has been recently introduced into the chemical pesticide industry to improve the properties of various control agents. One potential reason for applying this technology is to deliver the active ingredient of pesticides to the target areas, encapsulate pesticide molecules, control the release of active ingredients, and protect the active ingredient from degradation or rapid decomposition, which leads to the waste of large quantities of pesticides in the environment, sometimes exceeding 90% of the amount of pesticide used (Hayles *et al*., 2017). The toxic effect of nanoparticles depends on their size, geometric shape, physicochemical properties, and ability to adhere and form aggregates. They act as catalysts for the formation of toxic compounds because their toxic effect is mediated by ingestion and absorption through the intestinal walls, subsequently accumulating in fat tissue (Key *et al*., 2011).

The study seeks to identify effective and safer alternatives to chemical pesticides by exploring the use of natural plant extracts, specifically from *N. oleander*. This plant, found in tropical and subtropical regions, has significant agricultural and medicinal value due to its rich content of flavonoids, tannins, saponins, glycosides, oleandrin, and alkaloids. These components demonstrate anti-feeding, insect-repelling, and insecticidal properties, making *N. oleander* effective against various insect pests, including *T. granarium* (Ayouaz *et al*., 2023). Further studies are needed to investigate the effects of *N. oleander* leaf extracts on the mortality rates and life performance parameters of the hairy grain beetle, *T. granarium*. This research aims to prepare a biologically formulated nano-iron oxide preparation from the leaves of the *N. oleander* plant and examine the efficiency of various concentrations in impacting the biological aspects of *T. granarium* at different stages of its life cycle, using direct laboratory methods. This approach positions the extracts as a viable alternative to traditional pesticides (Islam *et al*., 2018; Ali & Sabit, 2023).

Materials and Methods

Preparation of aqueous extract for *Nerium oleander* L. leaves: Newly grown leaves of *N. oleander* L. were collected from the midrib of the plant in the gardens of the College of Science (Agricultural Research Garden) at the University of Baghdad in August. In the laboratory, leaves that were free from damage, insects, and fungal infestations were isolated. The leaves were thoroughly washed to remove any dust. 50 g of leaves were cut into small pieces and placed in an electric blender. Then, 100 ml of distilled water was added to the crushed leaves, covered, and left for 15 minutes. The resulting mixture was filtered using a Buchner funnel with Whatman No. 1 filter paper. The filtrate was then centrifuged to sediment any remaining fine plant particles and to obtain the crude extract, a thick, dark green liquid. The experiment was conducted at 25 °C, and the pH value of the aqueous extract from *N. oleander* leaves was measured and found to be 4. This extract was stored in tightly sealed, opaque glass bottles, with all relevant data recorded. Information about the plant sample was kept in a refrigerator at 4°C until needed (Harborne, 1973).

Synthesis of Fe_2O_3 nanoparticles: Iron oxide nanoparticles were biologically synthesized using the aqueous extract of *N. oleander* L., leaves. 100 ml of the aqueous extract was taken, and 5 g of Ferrous Sulfate Heptahydrate ($FeSO_4.7H_2O$), with a molecular weight of 278.01 g/mol and manufactured by LOBA CHEMIE (India), was added. The color of the aqueous extract changed from light green to black, indicating the formation of iron oxide nanoparticles. The mixture was placed in a Wise Shake for 24 hours, followed by stirring with a magnetic stirrer for an additional 1h to ensure thorough mixing. It was then distributed into 10 ml tubes and placed in a centrifuge set to 10,000 RPM for 20 minutes to precipitate the resulting iron oxide nanoparticles (Kiruba Daniel *et al*., 2013; Nawar *et al*., 2024).

After completing this process, the supernatant was discarded, and the precipitate was collected. The precipitate remained in the same plastic tubes, and then 5 mL of distilled deionized water was added. The tubes were placed back in the centrifuge at a speed of 10,000 RPM for 20 minutes to wash the precipitate. A dark-colored precipitate was obtained, indicating the presence of iron oxide nanoparticles (Fe_2O_3). The water was removed by spreading the precipitate in a thin layer on lab plates and placing them in an oven at 40°C for 24 minutes to dry. Once dried, the precipitate was collected and ground into a fine powder, representing Fe_2O_3 nanoparticles, and stored for future use (Kiruba Daniel *et al*., 2013; Nawar *et al*., 2024). To investigate the synthesis of iron oxide (Fe_2O_3) and analyze its particle characteristics, we conducted X-ray diffraction (XRD) using an X'Pert Pro system. The surface morphology was examined through field emission scanning electron microscopy (FE-SEM) and employed Energy Dispersive X-ray (EDX) to identify the presence of iron (Fe) and oxygen (O) in samples prepared using the aqueous extraction method from *N. oleander* leaves. Atomic force microscopy (AFM) was used to assess the roughness and mean diameter of the nanoparticles. Additionally, Fourier-transform infrared spectroscopy (FTIR) identified the functional groups and molecular structure (Nnadozie & Ajibade, 2020). A sample of the iron oxide nanoparticles was collected and sent to the Phi Nano Science Center (PNSC) in Baghdad, Iraq. The concentrations of nano iron oxide preparations for *N. oleander* leaves were created by dissolving 4 g of the powder in 1000 mL of deionized water to achieve a concentration of 4000 PPM. Other concentrations of 1000, 2000, and 3000 PPM were prepared using the same method. The control treatment consisted of deionized water only (Nawar *et al*., 2024).

Insect cultures: *T. granarium* was collected from infested wheat grains at the Storage Entomology Laboratory, Department of Plant Protection, College of Agricultural Engineering Sciences, University of Baghdad, in July. The infested grains were transferred to clean, sterilized 600 ml glass bottles. The insect was reared on wheat grains of the IPA 99 variety taken from the Al-Qadisiyah silo/General Company for Grain Trade/Ministry of Trade. Samples of wheat used for rearing were frozen at -20°C for 20 days to eliminate any potential infestation by storage pests. The samples were

placed in glass bottles, which were covered with organza fabric and secured with a rubber band. These bottles were then placed in a Binder-type incubator maintained at a temperature of 35 ± 1°C and a relative humidity of 45 ± 5%. A hygrometer was installed in the incubator, and to sustain the relative humidity level, 3 grams of KOH (potassium hydroxide) were added to 100 milliliters of water in sealed glass containers (Alvi *et al*., 2018).

The eggs were obtained by isolating 10 pairs of new adult insects (females and males) aged 1 to 2 days. For the experiments, 10 eggs were transferred for each replicate across three replicates for every treatment, including a control treatment. Larvae were produced from the hatched eggs, using 10 larvae per replicate. These larvae were 15 days old and also included three replicates for each treatment, plus a control. Newly formed pupae were monitored, with 10 pupae isolated per replicate at 24 h post-formation, again featuring three replicates for each treatment in addition to the control. For the adult stage, pairs of 24 hour males and females were selected from the emerged pupae, using 10 pairs per replicate and maintaining three replicates for each treatment as well as a control group (Hadi & Al-Khazraji, 2021). All insect life stages were treated with prepared concentrations of nano iron oxide, 1000, 2000, 3000, and 4000ppm for different time periods, 24, 48, and 72 h periods, and at varying temperatures, 25, 35, and 40 °C.

Iron oxide nanoparticles characterization

XRD analysis: X-ray diffraction is a powerful analytical technique used to determine the crystallographic structure, phase composition, and other structural properties of materials (Kumar, 2022). Fig. 1 shows the structure of the synthesis of Nano-iron oxide (Fe_2O_3).

The peaks of Fe_2O_3 in the hexagonal phase matched with JCPD card No. 098-5840, with Miller indices (012), (104), (110), (113), (202), (024), (116), (214), (217) at 2θ values of 24.12°, 33.11°, 35.61°, 40.82°, 43.48°, 49.41°, 54.00°, 62.96°, and 75.1°. XRD analysis confirmed that the reddish-brown Fe_2O_3 particles were magnetic, exhibited high crystallinity and purity, with a calculated crystal size of 26.5 nm using the Scherrer equation (Scherrer, 1918):

$$\text{Dhkl} = \frac{k \times \lambda}{\beta_{hkl}\, cos\theta}$$

where D is the crystalline size, which is perpendicular to the lattice plane, hkl is a Miller index, λ is the X-ray wavelength (1.5404°A), β is the line broadening at half the maximum intensity (FWHM), K is the dimensional shape factor of about 0.9, and θ is the Bragg angle.

FE-SEM analysis: Fig. 2 shows the surface morphology of iron oxide nanoparticles synthesized using aqueous extract from *N. oleander* leaves. The particles primarily exhibit a significant semispherical shape and tend to aggregate. This aggregation is commonly attributed to the presence of organic residues.

EDX analysis: The results of EDX analysis proved the formation of pure Nano-iron oxide, as shown in Table 1. This table illustrates the presence of oxygen and iron in the sample, with oxygen having a higher ratio than iron. Additionally, Fig. 3 shows that the chemical components are uniformly distributed.

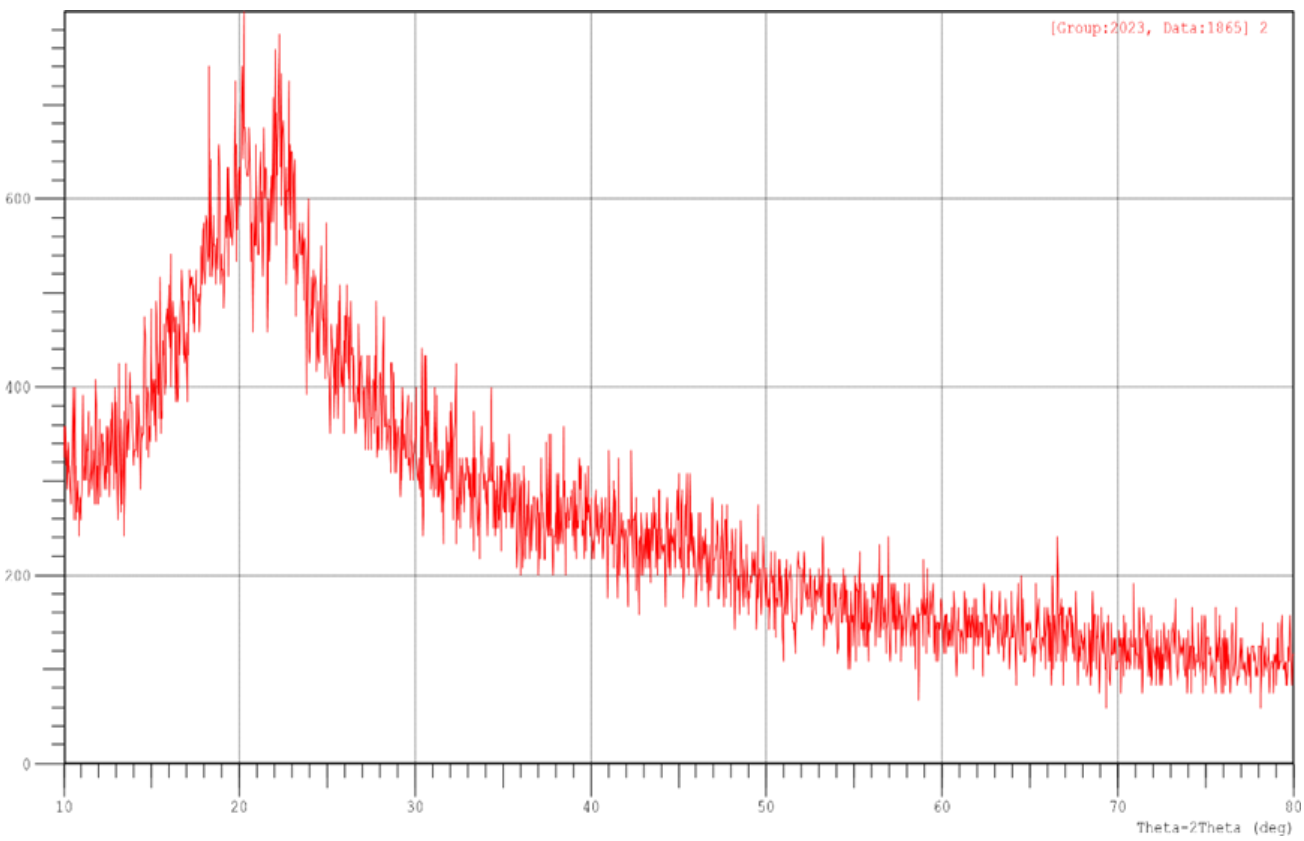

Fig. 1. XRD analysis of Fe_2O_3.

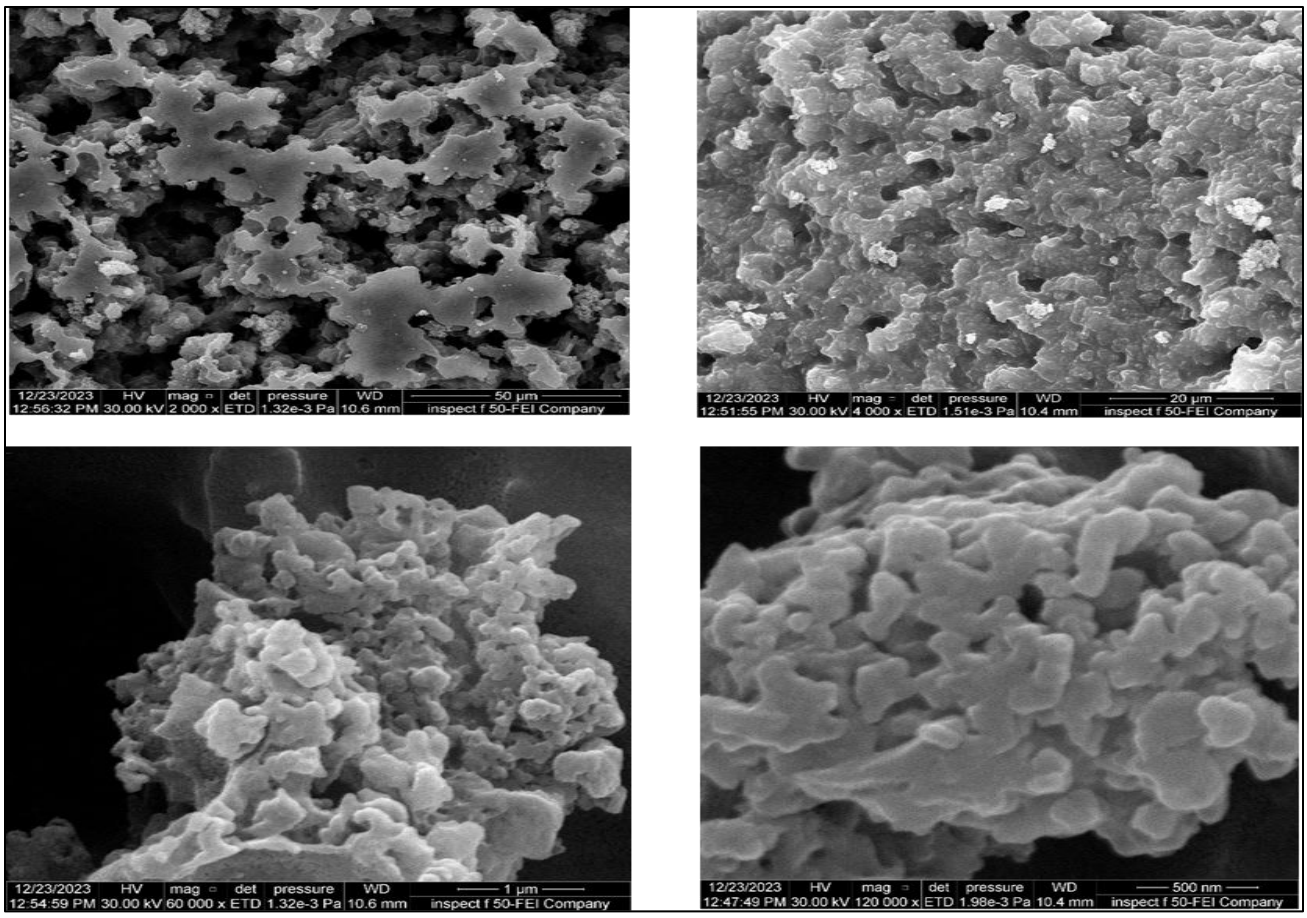

Fig. 2. FE-SEM analysis of Fe_2O_3.

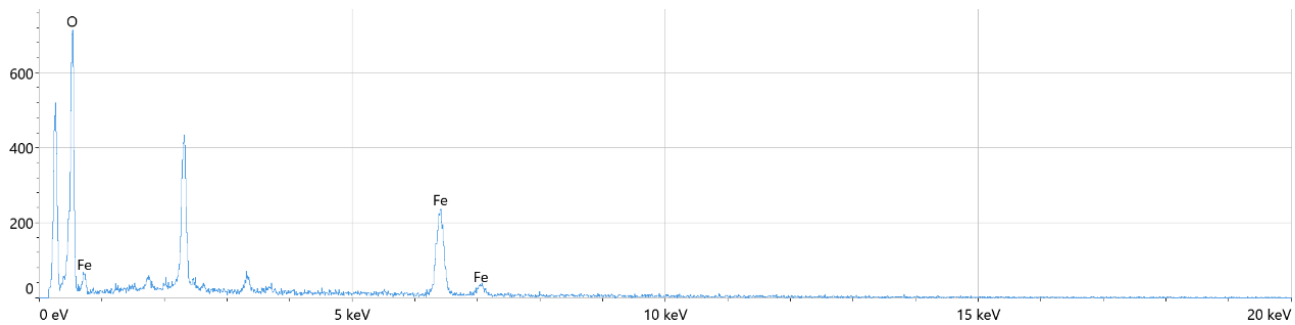

Fig. 3. EDX analysis of Fe_2O_3 nanoparticles.

Table 1. EDX analysis of Fe_2O_3 nanoparticles.

Element	Atomic %	Atomic % Error	Weight %	Weight % Error
O	86.7	1.5	65.0	1.1
Fe	13.3	0.4	35.0	1.1

AFM analysis: AFM provides 3D imaging of the sample surface, as shown in Fig. 4, and illustrates the distribution of Fe_2O_3 grains, which represents particle accumulation versus average mean diameter. The average mean diameter is typically around 47.94 nm with a spherical shape, which falls within the nanoscale range.

FTIR analysis: FTIR spectrum of Fe_2O_3 nanoparticles synthesized by aqueous leaf extract of *N. oleander* is shown in Fig. 5 and Table 2. Two weak peak at 3672.21- 3741.65 cm^{-1} appeared that due to (O-H) group of Alcohol, while strong peaks appeared in two positions, the first at 3402.00- 3519.85 cm^{-1} belongs to Amino acid (intermolecular bonds, O-H), and the second at 1041.49-1124.42 cm-1 belongs to Alcohol (C-O), Additionally, other peaks at different frequencies were medium, which were (2329.85-2360.71), (2933,53- 2966.31), (1631.67- 1722.31), (1215.07), (999.06), and (592.11) cm^{-1}. These positions belong to Carbon dioxide (O=C=O), Alkane (Methylene, C-H), Amine protein (N-O), Carboxylic acid (C=O), Ether (Hydrogen ester, C-O), Halogenated alkene group (C-Cl, and C=C), Alkane halogenated group (C-H-C, and C-Cl), respectively.

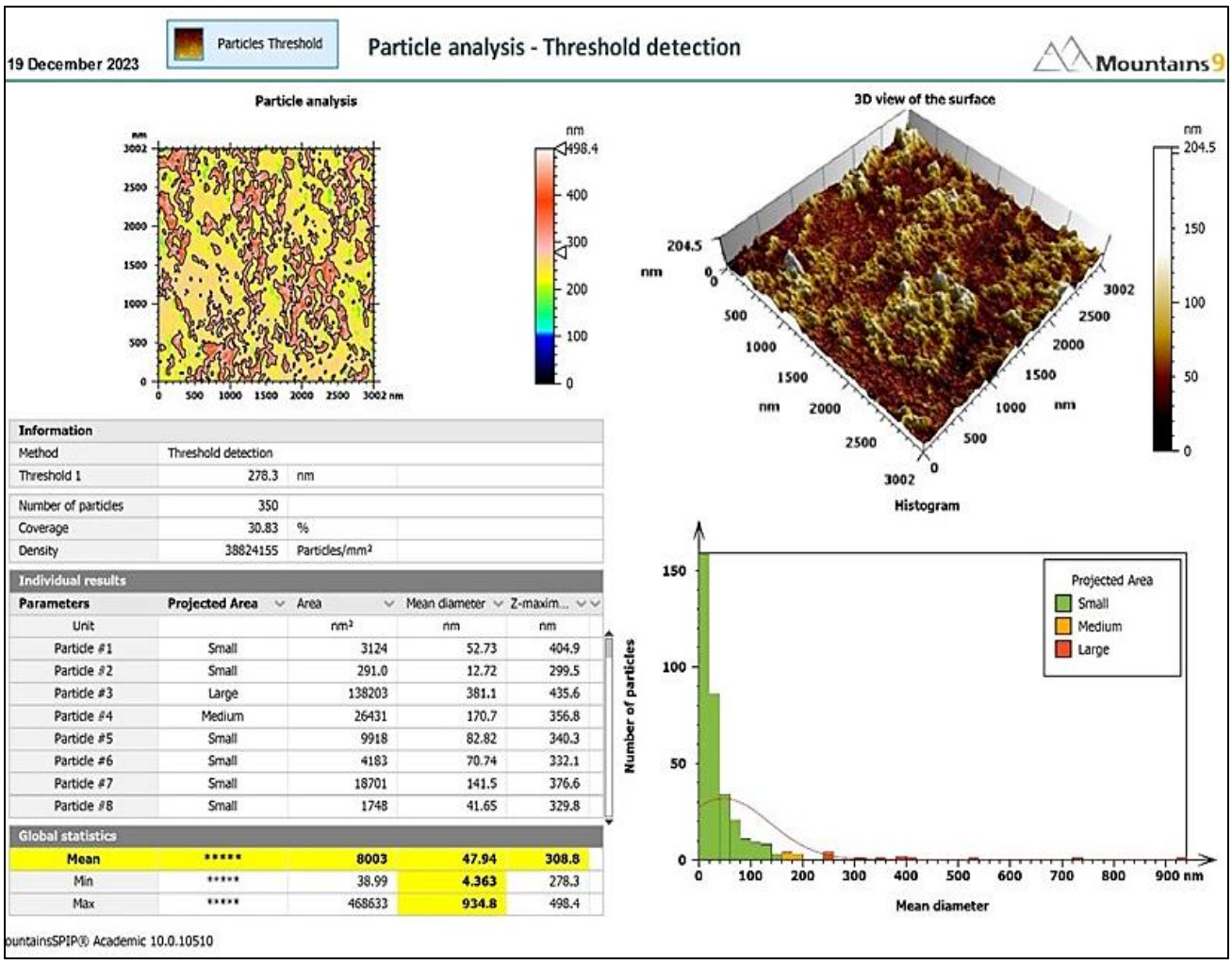

Fig. 4. AFM surface and Histogram for grain accumulation.

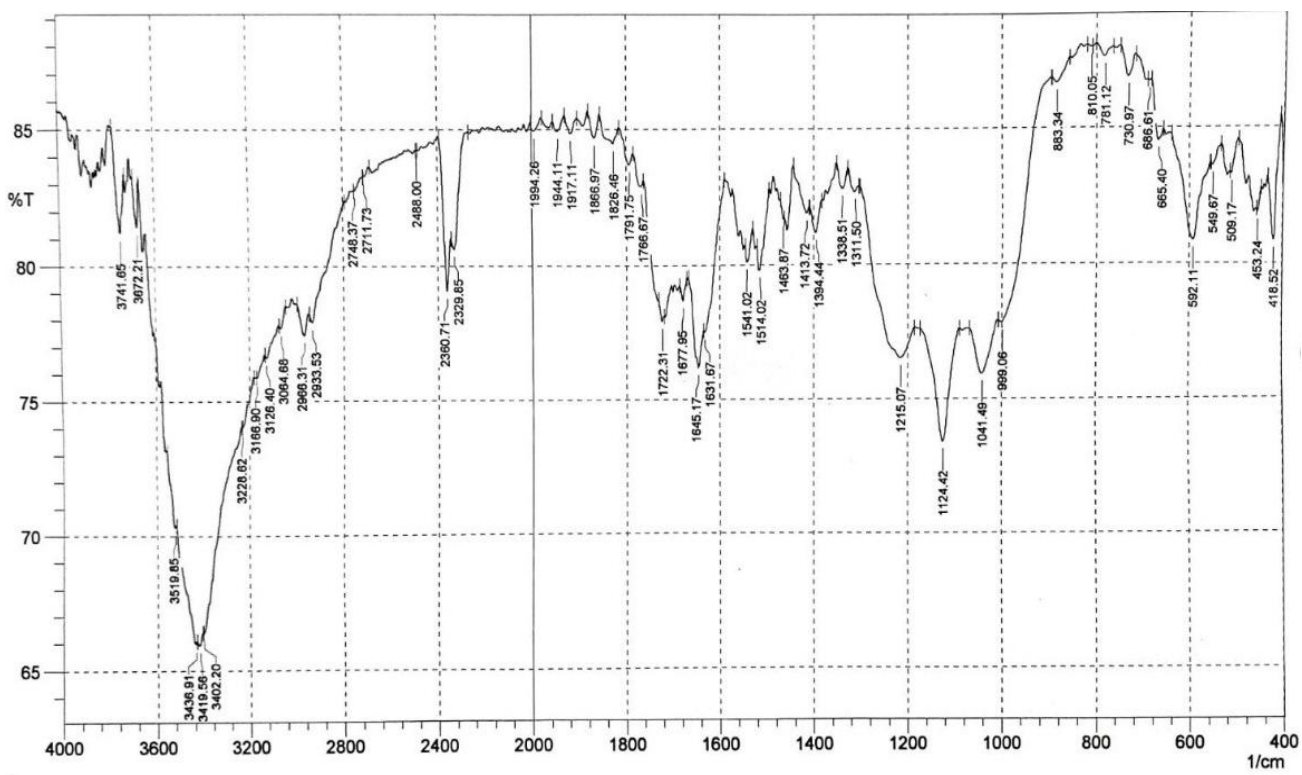

Fig. 5. FTIR spectroscopy Fe_2O_3 Nanoparticles.

Table 2. FTIR spectroscopy Fe_2O_3 nanoparticles.

No.	Frequency (Absorption) Cm^{-1}	Functional group	Compound class	Appearance
1.	3402.20 – 3519.85	O-H Stretching	Amino acid (Intermolecular Bonds)	Strong
2.	3672.21 – 3741.65	O-H Stretching	Alcohol	Weak
3.	2329.85 – 2360.71	O=C=O Stretching	Carbon Dioxide	Medium
4.	2933.53 – 2966.31	C-H Stretching	Alkane (Methylene)	Medium
5.	1631.67 – 1722.31	N-O Stretching C=O Stretching	Amin (protein) and Amide Carboxylic acid	Medium
6.	1215.07	C-O Stretching	Ether (Hydrogen ester)	Medium
7.	1041.49 – 1124.42	C-O Stretching	Alcohol	Strong
8.	999.06	C-Cl Bending C=C Bending	Halogenated Alkene	Medium
9.	592.11	C-H-C Stretching C-Cl Stretching	Alkane Halogenated	Medium
10.	418.52 – 999.06			Finger Print

Table 3. The effect of Fe_2O_3 nanoparticles on *T. granarium* egg inhibition.

Temp. ̊C	Conc. ppm	Mortality rate % Time (h) 24	48	72	Average Conc.
25	1000	0.00	0.00	0.00	0.00
	2000	0.00	0.00	6.66	2.22
	3000	9.66	13.33	18.33	13.77
	4000	33.33	46.66	87.00	55.66
35	1000	0.00	6.33	13.99	6.77
	2000	16.70	20.00	33.33	23.34
	3000	26.99	43.33	60.00	43.44
	4000	73.66	100.00	100.00	91.22
40	1000	13.33	16.70	23.33	17.79
	2000	23.99	36.66	43.33	34.66
	3000	30.00	46.66	70.00	48.89
	4000	93.66	100.00	100.00	97.89
Rate		26.78	35.81	46.33	---

LSD (0.05): Conc.= 12.73*, Time = 8.24* h, Interaction = 16.75*

Table 4. Direct effect of Fe_2O_3 nanoparticles on *T. granarium* larvae mortality.

Temp. ̊C	Conc. ppm	Mortality rate % Time (h) 24	48	72	Average Conc.
25	1000	26.66	33.33	50.00	36.66
	2000	30.00	43.33	56.66	43.33
	3000	33.33	56.66	63.66	51.22
	4000	80.00	93.33	100.00	91.11
35	1000	46.66	50.00	56.99	51.22
	2000	56.66	73.33	83.33	71.11
	3000	76.66	83.33	96.66	85.55
	4000	100.00	100.00	100.00	100.00
40	1000	66.66	76.66	83.33	75.55
	2000	76.66	79.99	96.66	84.44
	3000	100.00	100.00	100.00	100.00
	4000	100.00	100.00	100.00	100.00
Rate		66.11	74.16	82.27	---

LSD (0.05): Conc.= 9.73*, Time = 6.88* h, Interaction = 13.05*

Table 5. Direct effect of Fe_2O_3 nanoparticles on *T. granarium* pupae mortality.

Temp. °C	Conc. ppm	Mortality rate % Time (h)			Average Conc.
		24	48	72	
25	1000	0.00	0.00	0.00	0.00
	2000	0.00	0.00	3.33	1.11
	3000	19.66	23.33	29.99	24.33
	4000	36.00	44.99	50.00	43.66
35	1000	0.00	0.00	0.00	0.00
	2000	13.33	16.66	23.33	17.77
	3000	20.00	26.66	36.99	27.88
	4000	48.99	63.33	73.66	61.99
40	1000	16.66	23.33	30.00	23.33
	2000	33.33	39.99	43.33	38.88
	3000	40.00	53.33	66.66	53.33
	4000	73.33	97.66	100.00	90.33
Rate		25.11	32.44	38.11	---

LSD (0.05): Conc. = 9.54*, Time = 6.37* h, Interaction = 12.97*

Table 6. Direct effect of Fe_2O_3 nanoparticles on *T. granarium* adult mortality.

Temp. °C	Conc. ppm	Mortality rate % Time (h)			Average Conc.
		24	48	72	
25	1000	16.66	19.99	23.33	19.99
	2000	20.00	26.66	33.33	26.66
	3000	26.66	33.33	53.33	37.77
	4000	43.66	63.66	73.00	60.11
35	1000	20.00	23.33	26.66	23.33
	2000	33.33	46.66	59.99	46.66
	3000	40.00	46.66	70.00	52.22
	4000	100.00	100.00	100.00	100.00
40	1000	26.66	33.33	46.66	35.55
	2000	66.66	96.66	100.00	87.77
	3000	100.00	100.00	100.00	100.00
	4000	100.00	100.00	100.00	100.00
Rate		49.47	57.52	65.53	---

LSD (0.05): Conc. = 12.78*, Time = 8.92* h, Interaction = 17.05*

The FTIR analysis indicates that iron oxide nanoparticles exhibit high activity, which is influenced by the number of functional groups identified in the FTIR spectrum. These functional groups include bioactive species such as amines, amides, carboxylic acids, and halogenated compounds.

Statistical analysis

Statistical analysis was performed using a Completely Randomized Design (CRD) to study the interactions between temperature, concentration, and time. Significant differences between the mean values of the treatments were compared using the Least Significant Difference (LSD) method. At a probability level of $p<0.05$, the data were analyzed using the Statistical Analysis System (SAS) software (2018).

Results

Direct effect of iron oxide Nanoparticles on *T. granarium* egg hatching: The results of Table 3 showed the effect of direct treatment of Iron oxide nanoparticles on *T. granarium* egg hatch inhibition rate at concentrations of 1000, 2000, 3000, and 4000 ppm for periods of 24, 48, and 72 hours, and at all temperatures of 25, 35, and 40°C. The average inhibition rates at 25°C for the four concentrations were 2.22, 0.00, 13.77, and 55.66%, respectively. There was no effect of the nanomaterial at the concentration of 1000 ppm. However, the inhibition rates at 40°C were 17.79%, 34.66%, 48.89%, and 97.89%, respectively.

The inhibition rates at the three exposure periods were 26.78%, 35.81%, and 46.33%, respectively (Table 4). The highest effect was observed at a concentration of 4000 ppm at temperatures of 35 and 40°C for 72 hours, with an inhibition rate of 100%. The results of the statistical analysis revealed significant differences among all the treatments. And there is a direct relationship between egg inhibition rates, different concentrations, temperatures, and exposure periods.

Direct effect of Fe_2O_3 nanoparticles on *T. granarium* pupae mortality: The results of Table 5 showed the effect of Iron oxide nanoparticles on *T. granarium* pupae mortality at the specified concentrations, exposure periods, and all previously mentioned temperatures. The Nano-preparation had a weak efficacy in mortality of the pupae, with pupae mortality rates of 0.0%, 1.11%, 24.33%, and 43.66% at the respective concentrations and at 25°C. The

mortality rates were 23.33%, 38.88%, 53.33%, and 90.33% at 40°C. The highest mortality rates were recorded at a concentration of 4000 ppm and temperatures of 35 and 40°C. The pupa mortality rates at the three exposure periods were 25.11%, 32.44%, and 38.11%, respectively.

The results of the statistical analysis indicated significant differences between all treatments. The effectiveness of the iron oxide nanoparticles in the treated pupae of the Hairy grain beetle caused deformities and the emergence of incompletely developed pupae. which died during the molting process, leaving parts of the old cuticle attached to them. Additionally, pale white pupae appeared, having lost their ability to harden and darken. Intermediate stages occurred due to a disruption in the pupation process and the formation of the complete insect.

Direct effect of Fe_2O_3 nanoparticles on *T. granarium* adult: The results of Table 6 show the effect of direct treatment with iron oxide nanoparticles on the mortality of *T. granarium* adults at concentrations of 1000, 2000, 3000, and 4000 ppm for periods of 24, 48, and 72 hours, and at all temperatures of 25, 35, and 40°C. The nano-preparation demonstrated clear effectiveness in killing adult insects, with mortality rates of 19.99%, 26.66%, 37.77%, and 60.11% for the respective concentrations at 25°C. The effect of the Nano-preparation increased at 35°C, and the highest effectiveness of the Nano-preparation was at 40°C, with adult mortality rates of 35.55%, 87.77%, 100%, and 100%, respectively. The adult mortality rates at the three exposure periods were 49.47%, 57.52%, and 65.53%, respectively.

The statistical analysis results indicated significant differences among the various transactions. The data concluded that the preparation of iron nanoparticles from the leaves of the *N. oleander* plant, when treated at different temperatures and exposure durations, has influenced the mortality rates of the directly treated adults. Furthermore, the results demonstrated a direct relationship between these factors.

Discussion

FE-SEM analysis of the synthesized Fe_2O_3 nanoparticles mainly showed semi-spherical shapes with noticeable aggregation, consistent with previous reports by Aziz *et al*., (2020) and Biswal *et al*., (2020). Additionally, AFM analysis revealed spherical Fe_2O_3 nanoparticles with an average diameter of approximately 47.9 nm, within the nanoscale range. This result aligns with that of Hoffmann *et al*., (2022), who observed a similar result with iron oxide nanoparticles of 41.9 nm in size. FTIR analysis confirms the presence of functional groups in the crystalline iron oxide nanoparticles synthesized using aqueous N. oleander extract, which acts as a capping and stabilizing agent for the nanoparticles (Shawuti *et al*., 2021). The absorption bands observed in the fingerprint region (418.52–999.06 cm^{-1}) provide detailed information about the molecular structures and functional groups, including amines, amides, carboxylic acids, and halogenated compounds (Saod *et al*., 2024). The bioactive functional groups present in Fe_2O_3 nanoparticles enhance their chemical activity and stability, which contributes to their high efficacy across various applications (Mabasa *et al*., 2021; Khan *et al*., 2023). When applied to insects, these nanoparticles significantly inhibited egg hatching, with the effectiveness increasing at higher temperatures, as demonstrated in Table 3. This observation is consistent with the findings of Sabet & Sabr (2015). Additionally, these findings are consistent with the research by Ghormade *et al*., (2011) and Hayles *et al*., (2017), which indicated that nanoparticles effectively deliver adhesive materials, such as pesticides. This enhanced delivery method increases the surface area in contact with the target organisms, allowing for larger quantities of toxic chemicals to be administered at desired levels while releasing them in small amounts over extended periods, ultimately leading to the mortality of the targeted pests.

Furthermore, nanoparticles and their ions can potentially damage DNA due to their ability to penetrate natural openings in cells. Metallic nanoparticles vary in size based on the type of metal used and the biological material employed in their production. Their increased contact surface area with treated organisms—such as eggs, larvae, or adults—enhances their ability to penetrate and reach targeted sites in fetal tissue, which can lead to respiratory failure and, eventually, death (Rai *et al*., 2022). We conclude from our results that iron oxide nanoparticles, biosynthesized in leaves, significantly increased the inhibition of egg hatching. This effect can be attributed to the ability of the iron nanoparticles (Fe_2O_3), which are smaller than 50 nm, to coat the eggshell. This coating prevents the eggs from breathing and hinders the formation of the embryo (Van Nhan *et al*., 2016).

Campos *et al*., (2018) explained that encapsulating active compounds in nanoparticles can hinder the development and growth of larvae beyond the treated stages, as well as reduce their overall numbers. This slow and continuous release of active compounds enhances the effect without the need to increase concentration levels. Wakil *et al*., (2024) further indicated that temperatures of 30–35°C and 65% relative humidity were optimal for insect development, leading to shorter developmental periods compared to lower temperatures (e.g., 25°C). Thus, temperature control can be used in conjunction with other methods, such as chemical or physical controls, to effectively reduce pest resistance and improve overall control efficiency. The observed larval mortality may be attributed to the direct method's impact, where nanoparticles inhibit the enzyme acetylcholinesterase, leading to increased mortality rates (Hammed *et al*., 2023).

Adetuyi *et al*., (2024) suggested that nanoparticles can impact subsequent generations by damaging vital organs and gradually weakening the insects over time. These findings are consistent with those of Nawar *et al*., (2024), who reported that nanoparticles derived from *Dodonaea* leaves also have similar effects, at concentrations of 2, 5, and 10 ppm, causing pupal mortality rates of 70.8%, 83.3%, and 89.3%, respectively, in *Galleria mellonella*, compared to 0% in the control group. These treatments also prolonged the pupal cycle. Based on the data, we conclude that the effects of most treatment concentrations significantly influenced the larval stage. This could be explained by the semiconductor properties of biosynthesized iron oxide nanoparticles, which offer excellent conductivity and chemical stability, thereby disrupting the physiological activities within the insect's body (Patil *et al*., 2014; Ambika & Sundrarajan, 2015). This is consistent with what Hadi & Al-Khazraji (2021)

reached when evaluated the effectiveness of the Nano-hexane extract (encapsulated with chitosan) of the leaves of the Ban plant and the temperatures used.

The findings revealed that adult mortality rates increased with rising temperatures under direct exposure. At a concentration of 3000 ppm, 100% mortality was recorded at 25°C, 35°C, and 40°C. These results are consistent with the observations of Mishra *et al*., (2017), who reported physiological damage in *Drosophila melanogaster* following nanoparticle treatment, including loss of body hairs, dark abdominal spots, abnormal swelling, and damage to the melanin layer and wing sheaths. The observed temperature-dependent increase in mortality may be attributed to enhanced enzymatic activity, particularly that of membrane-bound enzymes regulating phospholipid layer permeability, which ultimately leads to insect death (Gunderson & Stillman, 2014).

Conclusion

The direct treatment of *T. granarium* with iron oxide nanoparticles, biosynthesized from the leaves of *N. oleander*, demonstrated a clear positive relationship among nanoparticle concentration, exposure duration, and applied temperature. The effects of these nanoparticles were more pronounced on the mobile stages of the insect (larvae and adults) compared to the non-mobile stages (eggs and pupae). This increased effectiveness can be attributed to the high toxicity of the nanoparticles, which results from their small size, geometric shape, and physicochemical properties, as well as their strong ability to adhere to the surfaces of the various insect stages. These nanoparticles act as toxic chemical catalysts by binding to insect circular proteins or accumulating in lipid tissues, forming harmful chemical compounds. Additionally, they disrupt the insect nervous system by inhibiting the acetylcholinesterase enzyme, which is responsible for transmitting nerve impulses. This disruption leads to various physiological disturbances, ultimately resulting in the death of the insect at various life stages.

Acknowledgments

We express our gratitude to the professors in the Department of Biotechnology and the Department of Protect Plant, University of Baghdad, especially Dr. Saad, Dr. Laith, Dr. Mustafa, Dr. Majid, and Mr. Azhar, for their valuable scientific contributions.

Conflict of Interest: The authors declare no conflict of interest.

Author's Contribution: Omar Hameed: Designed and conducted the experiments, analyzed data, and wrote the manuscript. Prof Dr. Ali Irfan: Supervised the research, guided the methodology, and reviewed the manuscript. Asst. Prof. Dr. Falah Abood**:** Assisted in data analysis and provided critical suggestions for improving the manuscript.

Reference

Adetuyi, B.O., P.A. Olajide, O.S. Omowumi and C.O. Adetunji. 2024. Application of plant-based nanobiopesticides as disinfectant. In: *Handbook of Agricultural Biotechnology* , 63-130. Wiley.

Alam, S.M. 1999. Nutrient uptake by plants under stress conditions. *Handbook of Plant and Crop Stress*. *2nd* ed, 285-313.

Ali, A.M. and F.A. Sabit. 2023. Eucalyptus and spearmint oils inhibit the biological activity of lesser grain borer and red flour beetles. *J. Aridland Agric*., 9: 138-143.

Alvi, A.M., N. Iqbal, M.A. Bashir, M.I.A. Rehmani, Z. Ullah, A. Latif and Q. Saeed. 2018. Efficacy of *Rhazya stricta* leaf and seed extracts against *Rhyzopertha dominica* and *Trogoderma granarium*. *Kuwait J. Sci.*, 45(3): 64-71.

Ambika, S. and M. Sundrarajan. 2015. Antibacterial behaviour of *Vitex negundo* extract assisted ZnO nanoparticles against pathogenic bacteria. *J. Photochem. Photobiol. B: Biol*., 146: 52-57.

Ayouaz, S., R. Arab, K. Mouhoubi and K. Madani. 2023. *Nerium oleander* Lin: A review of chemical, pharmacological and traditional uses. *J. Biomed. Res. Environ. Sci.*, 4(4): 641-650.

Aziz, W.J., M.A. Abid, D.A. Kadhim and M.K. Mejbel. 2020. Synthesis of iron oxide (β-Fe_2O_3) nanoparticles from Iraqi grapes extract and its biomedical application. *IOP Conf. Ser.: Mater. Sci. Eng.*, 881(1): 012099.

Biswal, S.K., G.K. Panigrahi and S.K. Sahoo. 2020. Green synthesis of Fe_2O_3-Ag nanocomposite using *Psidium guajava* leaf extract: An eco-friendly and recyclable adsorbent for remediation of Cr(VI) from aqueous media. *Biophys. Chem.*, 263: 106392.

Brent, J. 1998. *Charles Sanders Peirce (Enlarged Edition), Revised and Enlarged Edition: A Life*. Indiana University Press.

Campos, E.V.R., P.L.F. Proença, J.L. Oliveira, A.E.S. Pereira, L.N. de Morais Ribeiro, F.O. Fernandes, K.C. Gonçalves, R.A. Polanczyk, T. Pasquoto-Stigliani, R. Lima, C.C. Melville, J.F. Della Vechia, D.J. Andrade and L.F. Fraceto. 2018. Carvacrol and linalool co-loaded in β-cyclodextrin-grafted chitosan nanoparticles as sustainable biopesticide aiming pest control. *Sci. Rep*., 8(1): 7623.

Ferencz, L. and A. Balog. 2010. A pesticide survey in soil, water and foodstuffs from central Romania. Carpath. *J. Earth Environ. Sci*., 5(1): 111-118.

Ghormade, V., M.V. Deshpande and K.M. Paknikar. 2011. Perspectives for nano-biotechnology enabled protection and nutrition of plants. *Biotechnol. Adv*., 29(6): 792-803.

Gunderson, A.R. and J.H. Stillman. 2014. An affinity for biochemical adaptation to temperature. *J. Exp. Biol*., 217(24): 4273-4274.

Hadi, O.H.A. and H.I. Al-Khazraji. 2021. Efficiency of *Moringa oleifera* leaf extracts in protecting wheat grains from infection by the hairy grain beetle (KHAPRA) Trogoderma granarium. *Int. J. Agric. Stat. Sci*., 17(1): 1099-1109.

Hammed, A.A.A., H.I. Al Shammari and S.A. Kathiar. 2023. Effect of nanocapsules and extract of *Metarhizium anisopliae* in inhibiting acetylcholine esterase enzyme in *Musca domestica* larvae. *Baghdad Sci. J*., 21(1): 41-52.

Harborne, J.B. 1973. in *Phenolic Compounds.* In: *Phytochemical Methods*. *Springer Netherlands*, 33-88.

Hayles, J., L. Johnson, C. Worthley and D. Losic. 2017. Nanopesticides: a review of current research and perspectives. In new pesticides and soil sensors*. Elsevier*, 193-225.

Hoffmann, N., G. Tortella, E. Hermosilla, P. Fincheira, M.C. Diez, I.M. Lourenço, A.B. Seabra and O. Rubilar. 2022. Comparative toxicity assessment of eco-friendly synthesized superparamagnetic iron oxide nanoparticles (SPIONs) in plants and aquatic model organisms. *Minerals*, 12(4): 451.

Hübner, F. and E.K. Arendt. 2013. Germination of cereal grains as a way to improve the nutritional value: a review. *Crit. Rev. Food Sci. Nutr.*, 53(8): 853-861.

Islam, M.T., E.S. Ali, S.J. Uddin, S. Shaw, M.A. Islam, M.I. Ahmed, M. Chandra Shill, U.K. Karmakar, N.S. Yarla, I.N. Khan, M.M. Billah, M.D. Pieczynska, G. Zengin, C. Malainer, F. Nicoletti, D. Gulei, I. Berindan-Neagoe, A. Apostolov, M. Banach and A.G. Atanasov. 2018. Phytol: A review of biomedical activities. *Food Chem. Toxicol*., 121: 82-94.

Key, S.C.S., D. Reaves, F. Turner and J.J. Bang. 2011. Impacts of silver nanoparticle ingestion on pigmentation and developmental progression in Drosophila. *Atlas J. Biol.*, 1(3): 52-61.

Khan, F., N. Tabassum, G.J. Jeong, W.K. Jung and Y.M. Kim. 2023. Inhibition of mixed biofilms of *Candida albicans* and Staphylococcus aureus by β-caryophyllene-gold nanoparticles. *Antibiotics*, 12(4): 726.

Kiruba Daniel, S.C.G., G. Vinothini, N. Subramanian, K. Nehru and M. Sivakumar. 2013. Biosynthesis of Cu, ZVI, and Ag nanoparticles using *Dodonaea viscosa* extract for antibacterial activity against human pathogens. *J. Nanopart. Res*., 15(1): 1319.

Koul, O. 2008. Phytochemicals and insect control: An antifeedant approach. *Crit. Rev. Plant Sci*., 27(1): 1-24.

Kumar, M. 2022. XRD analysis for characterization of green nanoparticles: A mini review. Glob. *J. Pharm. Pharm. Sci*., 10(1).

Mabasa, X.E., L.M. Mathomu, N.E. Madala, E.M. Musie and M.T. Sigidi. 2021. Molecular spectroscopic (FTIR and UV-Vis) and hyphenated chromatographic (UHPLC-qTOF-MS) analysis and *In vitro* bioactivities of the *Momordica balsamina* leaf extract. *Biochem. Res. Int*., 2021: 1-12.

Mansoor-ul-Hasan, M.S., A. Ullah, W. Wakil and A. Javed. 2006. Response of *Trogoderma granarium* (Everts) to different doses of *Haloxylon recurvum* extract and deltamethrin. *Pak. Entomol*., 28(2): 25-30.

Mishra, M., D. Sabat, B. Ekka, S. Sahu and P. Dash. 2017. Oral intake of zirconia nanoparticle alters neuronal development and behaviour of *Drosophila melanogaster*. *J. Nanopart. Res.*, 19(8): 282.

Nnadozie, E.C. and P.A. Ajibade. 2020. Green synthesis and characterization of magnetite (Fe_3O_4) nanoparticles using *Chromolaena odorata* root extract for smart nanocomposite. *Mater. Lett*., 263: 127145.

Patil, R.S., M.R. Kokate, D.V. Shinde, S.S. Kolekar and S.H. Han. 2014. Synthesis and enhancement of photocatalytic activities of ZnO by silver nanoparticles. Spectrochim. *Acta Mol. Biomol. Spectrosc*., 122: 113-117.

Rai, P., V. Pratap Singh, S. Sharma, D.K. Tripathi and S. Sharma. 2022. Iron oxide nanoparticles impart cross tolerance to arsenate stress in rice roots through involvement of nitric oxide. *Environ. Pollut*., 307: 119320.

Rajendran, S. and S.C. Anand. 2002. Developments in medical textiles. *Text. Prog.*, 32(4): 1-42.

Sabet, F.A. and S.H. Sabr. 2015. Evaluation of the efficacy of ozone and high temperature to control eggs and pupae stages in laboratory for hairy grain beetle (KHAPRA) *Trogoderma granarium* Everts Coleoptera: Dermestidae. *Iraq. J. Sci*., 56(3B): 2164-2169.

Sabit, F.A., M.A.L.I. Abdullah and S.A.K. Elhadeeti. 2025. Study of the contact effect of stearic acid on *Trogoderma granarium* Everts, 1898 (Coleoptera: Dermestidae) in the laboratory. *Asian J. Agric*., 9(1): 185-190.

Saod, W.M., M.S. Al-Janaby, E.W. Gayadh, A. Ramizy and L.L. Hamid. 2024. Biogenic synthesis of iron oxide nanoparticles using Hibiscus sabdariffa extract: Potential for antibiotic development and antibacterial activity against multidrug-resistant bacteria. *Curr. Res. Green Sustain. Chem*., 8: 100397.

SAS Institute. 2018. SAS/STAT User's Guide, version 2018. SAS Institute, Cary, NC.

Saxena, R.C., O.P. Dixit and V. Harshan. 1992. Insecticidal action of *Lantana camara* against *Callosobruchus chinensis* (Coleoptera: Bruchidae). *J. Stored Prod. Res*., 28(4): 279-281.

Scherrer, P. 1918. Bestimmung der Grosse und inneren Struktur von Kolloidteilchen mittels Röntgenstrahlen. *Nach Ges. Wiss. Göttingen,* 2: 8-100.

Semple, R.L. 1992. *Towards integrated commodity and pest management in grain storage*. FAO, Rome, Italy, 180.

Shawuti, S., C. Bairam, A. Beyatlı, İ.A. Kariper, I.N. Korkut, Z. Aktaş, M.O. Öncül and S.E. Kuruca. 2021. Green synthesis and characterization of silver and iron nanoparticles using *Nerium oleander* extracts and their antibacterial and anticancer activities. *Plant Introd*., 91(92): 36-49.

Stathas, I.G., A.C. Sakellaridis, M. Papadelli, J. Kapolos, K. Papadimitriou and G.J. Stathas. 2023. The effects of insect infestation on stored agricultural products and the quality of food. *Foods*, 12(10): 2046.

Van Nhan, L., C. Ma, Y. Rui, W. Cao, Y. Deng, L. Liu and B. Xing. 2016. The effects of Fe_2O_3 nanoparticles on physiology and insecticide activity in non-transgenic and Bt-transgenic cotton. *Front. Plant Sci*., 6: Article 1263.

Wakil, W., N.G. Kavallieratos, N. Eleftheriadou, S.A. Haider, M.A. Qayyum, M. Tahir, K.G. Rasool, M. Husain and A.S. Aldawood. 2024. A winning formula: sustainable control of three stored-product insects through paired combinations of entomopathogenic fungus, diatomaceous earth, and lambda-cyhalothrin. *Environ. Sci. Pollut. Res*., 31(10): 15364-15378.